JPE 17-2-13

https://doi.org/10.6113/JPE.2017.17.2.442
ISSN(Print): 1598-2092 / ISSN(Online): 2093-4718

# Modeling and a Simple Multiple Model Adaptive Control of PMSM Drive System

Taesu Kang[*], Min-Seok Kim[**], Sa Young Lee[***], and Young Chol Kim[†]

[*]Modeling & Simulation team, Defense R&D Center, Hanwha Corporation , Daejeon, Korea
[**]Central Research Institute, Korea Hydro & Nuclear Power Co., Ltd, Daejeon, Korea
[***]Department of Electrical Engineering, Myongji College, Seoul, Korea
[†]Department of Electronics Engineering, Chungbuk National University, Cheongju, Korea

## Abstract

This paper deals with the input-output modeling of a vector controlled PMSM drive system and design of a simple multiple model adaptive control (MMAC) scheme with desired transient responses. We present a discrete-time modeling technique using closed-loop identification that can experimentally identify the equivalent models in the *d*-*q* coordinates. A bank of linear models for the equivalent plant of the current loop is first obtained by identifying them at several operating points of the current to account for nonlinearity. Based on these models, we suggest a simple *q*-axis MMAC combined with a fixed *d*-axis controller. After the current controller is designed, another equivalent model including the current controller in the speed control loop shall be similarly obtained, and then a fixed speed controller is synthesized. The proposed approach is demonstrated by experiments. The experimental set up consists of a surface mounted PMSM (5 KW, 220V, 8 poles) equipped with a flywheel load of 220kg and a digital controller using DSP (TMS320F28335).

**Key words:** Closed-loop identification, Discrete-time characteristic ratio assignment (DCRA), Multiple model adaptive control (MMAC), Permanent magnet synchronous motor

## I. Introduction

Permanent magnet synchronous motors (PMSM) are widely used in the manufacturing industry, robot systems, and in many other applications because of their excellent features such as high efficiency, low cost, minimal maintenance, and high power density. To achieve good performance when the load and speed command vary, various design methods for PMSM speed control have been developed [1], [2], and references therein]. In most non-adaptive methods, all the parameters of the PMSM model must be previously obtained to design a controller analytically [3]. However, it is not easy to identify certain parameters (e.g., inertia and friction coefficient) precisely. A disadvantage of adaptive schemes is that the adaptation algorithm may be very sensitive to outliers of the measured data in the recursive process and this can result in poor performance.

Unlike typical adaptive control based on real-time parameter tuning, multiple model adaptive control (MMAC) [4], [5] uses a bank of linearized models and a family of candidate controllers. These models can be obtained from N operating points in advance. The controller is also a priori designed for each model of the model bank. At every recursive step, the probability that each model represents the dynamics of the actual plant is calculated. Then weights are determined using these probabilities. These weight factors are multiplied by $N$ control inputs such that the more probable models carry more weight. The resulting controller output is represented by a linear combination of weighted control inputs. The MMAC scheme is to find a proper interpolation of the outputs of predesigned controllers instead of real-time parameter adaptation. The idea of MMAC was proposed by Lainiotis [4]. It has been used for the control of aircraft [6] and for robust damping control of power system [7].

Manuscript received Sep. 3, 2016; accepted Jan. 22, 2017
Recommended for publication by Associate Editor Shihua Li.
[†]Corresponding Author: yckim@cbu.ac.kr
Tel: +82-43-261-2475, Fax: +82--43-268-2386, Chungbuk Nat'l Univ.
[*]Modeling & Simulation team, Defense R&D Center, Hanwha Corp., Korea
[**]Central Research Inst., Korea Hydro & Nuclear Power Co., Ltd, Korea
[***]Department of Electrical Engineering, Myongji College, Korea

In many industrial applications of the PMSM drive system, the reference input is usually given as a step or ramp for a specific period of time. While the operating conditions are kept constant, the plant parameters do not change much. During this period, it is not necessary to identify all the parameters in real time. Therefore, in such cases, the MMAC scheme is more advantageous than parameter adaptive methods.

In this paper, we present a discrete-time MMAC for a PMSM drive system so that the resulting system satisfies the transient response specifications over the full speed range.

The adjustable speed drive system of the vector controlled PMSM mainly consists of two control loops: the current loop and the speed loop. The dynamics of the PMSM generally change with speed and load variations. In MMAC, this nonlinearity is captured by a set of linearized models. Since the rotor speed and the electromagnetic torque are dominantly related to the *q*-axis current and not much to the *d*-axis current, the equivalent plant of the *q*-axis current loop can be represented as a bank of linearized models. The dynamics of the current loop has a much faster mode than the speed-control loop due to a large moment of inertia. Therefore, it is assumed that the nonlinearity of the speed control loop can be ignored. After all, we need to identify three kinds of models: *q*-axis models, a *d*-axis model, and a speed model.

Since an open-loop identification method cannot be applied to empirical modeling of the vector-controlled PMSM drive system, a closed-loop identification (CLID) method [7, 8] is employed in this approach. CLID is used for situations in which the plant has an integrator or it is unstable, and it is neither possible nor recommended to open the loop to acquire data for the identification. To apply the CLID method, it is necessary to design an initial controller that stabilizes the closed-loop system.

The speed-control loop is first open and identifies the models of the *q*-axis and *d*-axis current loops. The speed loop should be modeled after the current controller is designed because the current-control system must be included in the speed model.

Once models are obtained, the remaining problem is to design each controller that satisfies the given transient response specifications. The discrete- time characteristic ratio assignment (DCRA) [11]-[13] is used for this purpose. DCRA is a model matching method in the sense that the controller is designed such that the resulting closed-loop transfer function matches the prescribed reference model. In [10]-[12], it was shown that a reference model satisfying the desired transient response can be generated easily by choosing two specific parameters, namely, the characteristic ratio and generalized time constant. DCRA is similar to the pole assignment method. However, it specifies the desired characteristic parameters instead of selecting the desired poles.

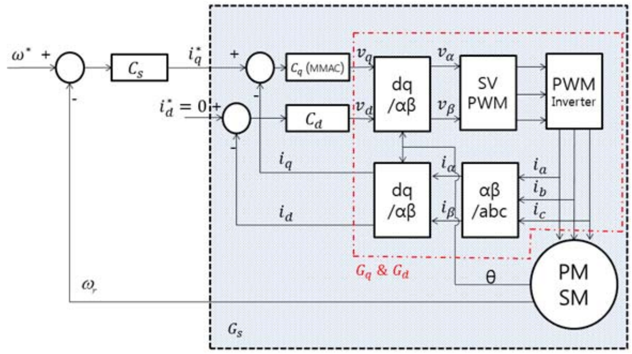

Fig. 1. Block diagram of the PMSM control system.

Direct digital control of PMSM based on such closed-loop experimental modeling has been proposed recently in [14]. In this work, we attempt to improve the performance of the previous work in [14] by introducing MMAC for the *q*-axis current controller. In particular, we will show that the proposed controller is useful for the case that its reference input changes stepwise between low speed and high speed.

The proposed approach was demonstrated by experiments. The experimental setup consisted of a surface mounted PMSM (5 KW, 3$\phi$ 220V, 8 poles, Higen Co.) equipped with a flywheel load of 220kg and a digital controller using DSP (TMS320F28335). Modeling and design procedures will be presented step by step. Experiments for both current tracking and speed control were carried out. The results showed that the MMAC algorithm has good transient controls despite its simple implementation structure.

## II. INPUT-OUTPUT MODELING OF PMSM

### A. *PMSM Control System in* $dq$ *Frame and Formulation of Modeling*

The design procedure is based on the vector control framework, as shown in Fig. 1. The mathematical model of a surface-mounted PMSM is represented in the rotational two-phase frame as follows:

$$v_d = R_s i_d + L_d \frac{di_d}{dt} - L_q \omega_r i_q , \tag{1}$$

$$v_q = R_s i_q + L_q \frac{di_q}{dt} + L_d \omega_r i_d + \omega_r \psi_m , \tag{2}$$

$$J \frac{d\omega_r}{dt} = K_t i_q - T_L - B\omega_r , \tag{3}$$

where $i_d$ and $i_q$ denote the $d$ -axis and $q$ -axis stator currents, respectively, and $v_d$ and $v_q$ denote the $d$ -axis and $q$ -axis stator voltages, respectively. The resistance and inductance of the stator coil are denoted by $R_s$ and $L_d$ ($L_q$), respectively. Here $\omega_r$ is the rotor angular velocity; $T_L$ is the load torque; $\psi_m$ is the flux linkage; and $J$, $K_t$, and $B$ denote the rotor inertia, torque constant, and viscous friction coefficient, respectively.

Currents $i_\alpha$ and $i_\beta$ are obtained by taking the Clarke transformation of three phase line currents of the PMSM, and then the Park's transformation of $i_\alpha$ and $i_\beta$ yields $i_d$ and $i_q$, respectively. Here $C_q$, $C_d$, and $C_s$ denote the $q$-axis and $d$-axis current controllers, and the speed controller to be designed, respectively. In this approach, $C_q$ is implemented by an MMAC while $C_d$ and $C_s$ are of a fixed digital controller.

To begin with, a brief overview of the proposed MMAC for a PMSM drive system is given. It is well known that rotor speed and electromagnetic torque are dominantly related to the $q$-axis current rather than the $d$-axis current. Therefore, we suppose that the nonlinearity of the PMSM dynamics can be represented by a set of linearized $q$-axis models and a single $d$-axis model. Each of the multiple models represents a model at one operating point of the $q$-axis current. All these models are identified by using the CLID method [9], [14]. These identified $q$-axis models constitute a model bank in the MMAC. Then a digital controller is designed for each model of the bank to satisfy the desired transient response. The weighting factors must be calculated in real time to indicate how close the current plant is to the individual model. Then the adaptive control input is obtained by a weighed linear combination of the controller's outputs. A digital controller for the $d$-axis current loop is also designed for a single $d$-axis model. The details of the MMAC scheme are given in Section III.

The second stage is to identify the equivalent model for the speed-control loop. The nonlinear dynamics of the speed-control loop is assumed to be negligible if the settling time of the current-control loop is sufficiently short compared with the speed loop. Thus, the equivalent plant of the speed-control loop can be represented by a single linear model. This model is similarly identified by using the CLID method. Then, the speed controller is designed for the model.

In this section, we concentrate on the experimental modeling of equivalent plants of the PMSM drive system. We will obtain three kinds of models (see Fig. 1): (i) a set of $q$-axis models $G_q$ from $v_q$ to $i_q$ in the current loop, (ii) a *d-axis* model $G_d$ from $v_d$ to $i_d$, and (iii) a model $G_s$ from $i_q^*$ to $\omega_r$ in the speed-control loop. Details are given in next subsections.

### *B. Experimental Modeling of the Equivalent Plants in the Current Loop*

Since the dynamics of current loop is not affected by the speed controller, modeling of the equivalent plant of the current loop can be performed regardless of the speed-control loop. All the components connected from $v_q$ to $i_q$ in the current loop are characterized as a discrete-time linear transfer function model at one operating condition. To capture nonlinearity by a set of linearized models, we divide the $q$-axis current appropriately into N in the rated current range and define them as operating points. Neglecting the interconnection between the $d$- and $q$-axes, the nonlinear dynamics of the PMSM can be covered by $N$ discrete-time linearized models, $G_q$.

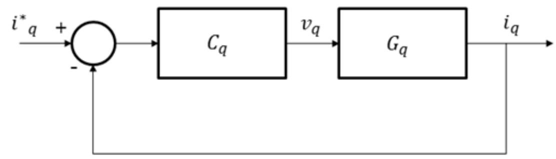

Fig. 2. Equivalent model of the *q-axis* current loop.

If the speed-control loop is open, as shown in Fig. 1, the $q$-axis current loop can be expressed by a single feedback control system including a set of discrete-time linear time-invariant (LTI) plants $G_q$, as shown in Fig. 2.

These models $G_q$ are identified at the preselected operating points using the CLID method. As a CLID algorithm, the closed-loop output error (CLOE) method proposed by Landau and Karimi [8], [9] is used in this approach.

The discrete-time $q$-axis model $G_q$ is defined as

$$\hat{G}_q(z^{-1}) := \frac{i_q}{v_q} = \frac{\hat{B}_q(z^{-1})}{\hat{A}_q(z^{-1})}, \tag{4}$$

where

$$\hat{A}_q(z^{-1}) = 1 + \hat{a}_{q1} z^{-1} + \cdots + \hat{a}_{naq} z^{-naq},$$
$$\hat{B}_q(z^{-1}) = \hat{b}_{q1} z^{-1} + \cdots + \hat{b}_{nbq} z^{-nbq}.$$

If we consider the two-parameter configuration for $C_q$, the CLOE identification can be illustrated by the block diagram shown in Fig. 3, where $r_o$ is one of the $N$ reference currents $i_q^*$'s. That is, $r_o$ is the reference current corresponding to each operating point. The input $r_t$ is the external excitation superposed onto $r_o$ for identification. This test input is usually chosen by a pseudo random binary sequence (PRBS).

To correctly identify the steady state gain of the plant model, the maximum pulse duration of the PRBS must be greater than the rise time of the plant. Furthermore, to cover the entire frequency spectrum generated by a particular PRBS, the length of test must be longer than the length of the sequence, $(2^c - 1)T_s$, where c is the number of cells and $T_s$ is the sampling time. It is recommended that the magnitude of the PRBS be selected from 0.5% to 10% of the operating point [9].

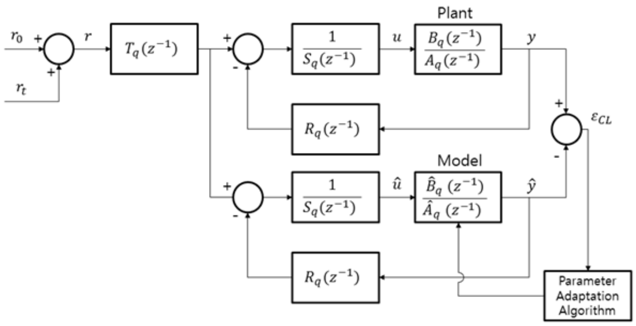


Fig. 3. Closed-loop output error identification method.

The two-parameter digital controller is represented in terms of three polynomials { $R_q$, $S_q$, $T_q$ } as shown in Fig. 3; therefore, it is also referred to simply as the RST controller [9]. Before applying the CLOE to the $q$ axis current loop, we select initial current controllers for both $C_q$ ( $R_q$, $S_q$, $T_q$ ) and $C_d$ ( $R_d$, $S_d$, $T_d$ ) that stabilize the closed loop system. It is not difficult to tune such a controller.

Letting $y(k) := i_q(k)$ , the closed loop system is

$$y(k+1) = -\{A_q(q^{-1}) - 1\}y(k) + B_q(q^{-1})u(k-d) + e(k) \tag{5}$$

$$S_q(q^{-1})u(k) = T_q(q^{-1})r(k) - R_q(q^{-1})y(k) \tag{6}$$

The recursive adaptation algorithm of the CLOE method is given as

$$\begin{gathered}\hat{\theta}(k+1) = \hat{\theta}(k) + F(k)\phi(k)\varepsilon_{CL}(k+1) \\ F(k+1) = \lambda_1(k)F(k)^{-1} + \lambda_2(k)\phi(k)\phi(k)^T, \\ (0 \le \lambda_1 \le 1; \quad 0 \le \lambda_2 \le 2) \\ \varepsilon_{CL}(k+1) = y(k+1) - \hat{y}(k+1) \\ \hat{y}(k+1) = \hat{\theta}(k)^T \phi(k)\end{gathered} \tag{7}$$

where

$$\hat{\theta}(k)^T := [\hat{a}_{q1}(k), \cdots, \hat{a}_{naq}(k), \hat{b}_{q1}(k), \cdots, \hat{b}_{nbq}(k)]$$

$$\phi(k)^T := [-\hat{y}(k), \cdots, \hat{y}(k-na+1), \hat{u}(k-1), \cdots, \hat{u}(k-nb+1)]$$

$$\hat{y}(k+1) := -\{\hat{A}_q(k, q^{-1}) - 1\}\hat{y}(k) + \hat{B}_q(k, q^{-1})\hat{u}(k)$$

$$S_q(q^{-1})\hat{u}(k) := T_q(q^{-1})r(k) - R_q(q^{-1})\hat{y}(k).$$

Applying a reference input $r_o$ and a PRBS test input $r_t$ to the PMSM system, the sampled data of { $y(k), r(k)$ } are measured experimentally. Then the CLOE algorithm (7) results in the estimated parameters of the model (4). Repeating this procedure with different operating points, $N$ $q$-axis models are obtained.

As mentioned earlier, since the $d$-axis reference current $i_d^*$ is always set to zero regardless of the motor speed, the $d$-axis plant does not need to be considered as multiple models. Thus the $d$-axis current loop can be expressed as a single feedback control system with discrete-time LTI plants $G_q$ , as shown in Fig. 4.

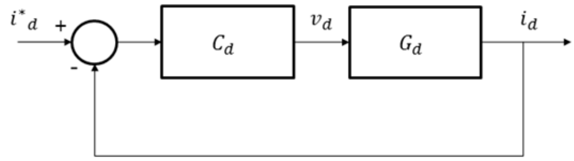


Fig. 4. Equivalent model of the $d$-*axis* current loop.

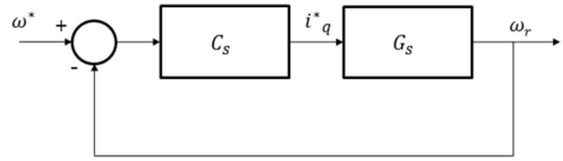


Fig. 5. Equivalent speed-control system.

Similar to the previous case, a discrete-time linearized model $\hat{G}_d$ can be identified by superposing the test input $r_t$ onto $i_d^*$ . The model $\hat{G}_d$ is defined as

$$\hat{G}_d(z^{-1}) := \frac{i_d}{v_d} = \frac{\hat{B}_d(z^{-1})}{\hat{A}_d(z^{-1})}, \tag{8}$$

where

$$\hat{A}_d(z^{-1}) = 1 + \hat{a}_{d1}z^{-1} + \cdots + \hat{a}_{nad}z^{-nad},$$

$$\hat{B}_d(z^{-1}) = \hat{b}_{d1}z^{-1} + \cdots + \hat{b}_{nbd}z^{-nbd}.$$

## C. *Experimental Modeling of the Equivalent Plant in the Speed-Control Loop*

Suppose that the current controllers, $C_q$ and $C_d$ , have been designed based on the identified $d$- and $q$-*axis* models. Methods for designing the controllers will be described in Section III. Then, the speed-control system of PMSM in Fig.1 can be represented by a single loop feedback system, as shown in Fig. 5, where $G_s$ denotes an equivalent model from $i_q^*$ to $\omega_r$ . Note that the entire current-control loops are included in the model $G_s$ .

We can see that $G_s$ can be identified in the same way as $G_q$ .

An identified model of the discrete-time plant $\hat{G}_s$ is defined as

$$\hat{G}_s(z^{-1}) = \frac{\hat{B}_s(z^{-1})}{\hat{A}_s(z^{-1})}, \tag{9}$$

where

$$\hat{A}_s(z^{-1}) = 1 + \hat{a}_{s1}z^{-1} + \cdots + \hat{a}_{nas}z^{-nas},$$

$$\hat{B}_s(z^{-1}) = \hat{b}_{s1}z^{-1} + \cdots + \hat{b}_{nbs}z^{-nbs}.$$

To acquire the input-output data, we need to select an initial speed controller $C_s^o$ that stabilizes the closed loop system. From Figs. 3 and 5, if we let $y(k) := \omega(k)$ , $r_o(k) := \omega^*(k)$ , and use an RST-type controller for $C_s$ , the same CLOE algorithm as (7) can be applied to the

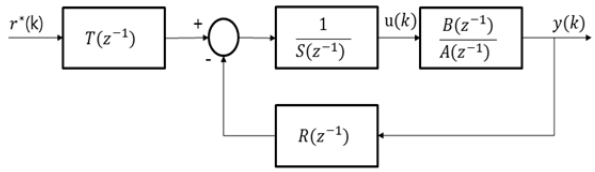


Fig. 6. Feedback system with two-parameter controller.

identification of $\hat{G}_s$. A PRBS test input $r_t$ is superposed onto the reference speed $r_o(k) := \omega^*(k)$. Finally, this model is used for the analytic design of the speed controller.

So far, it has been shown that a PMSM system with a vector controller can be converted into three independent single loop feedback systems, as shown in Figs. 2, 4, and 5. Experimental demonstrations of these modeling procedures will be described in Section IV.

## III. A Simple MMAC and Digital Control of PMSM with Time Responses

In this section, we describe how to design a digital controller of PMSM to satisfy the transient response specifications such as the maximum overshoot and settling time. The *d*-axis current controller and the speed controller are of a single feedback controller. On the other hand, the *q*-axis current controller $C_q$ is designed with the MMAC scheme.

In MMAC, the candidate controller corresponding to an individual model of the plant model bank must be synthesized in advance. To achieve the desired transient responses, all these controllers are designed using the DCRA method [10], [12]. We first present the design method of the two-parameter digital controller using DCRA, followed by MMAC design.

### *A. Direct Design of Two-Parameter Controllers for $C_d$ and $C_s$*

Consider the typical discrete-time feedback control system shown in Fig. 6, where an LTI plant and an two-parameter controller are described by

$$\frac{B(z^{-1})}{A(z^{-1})} = \frac{b_1 z^{-1} + b_2 z^{-2} + \cdots + b_{nb} z^{-nb}}{1 + a_1 z^{-1} + a_2 z^{-2} + \cdots + a_{na} z^{-na}}, \tag{10}$$

$$S(q^{-1})u(k) = T(q^{-1})r(k) - R(q^{-1})y(k), \tag{11}$$

where

$$S(z^{-1}) = 1 + s_1 z^{-1} + \cdots + s_{ns} z^{-ns},$$
$$R(z^{-1}) = r_0 + r_1 z^{-1} + \cdots + r_{nr} z^{-nr},$$
$$T(z^{-1}) = t_0 + t_1 z^{-1} + \cdots + t_{nt} z^{-nt}.$$

If the plant model $B(z^{-1}) / A(z^{-1})$ is $\hat{G}_d$ (or $\hat{G}_s$) and the corresponding controller is $C_d$ (or $C_s$) of the RST type, the feedback system in Fig. 6 is equivalent to the system in Fig. 4 (or Fig. 5). The closed-loop system is given by

$$H(z^{-1}) = \frac{T(z^{-1})B(z^{-1})}{A(z^{-1})S(z^{-1}) + B(z^{-1})R(z^{-1})} = \frac{T(z^{-1})B(z^{-1})}{P(z^{-1})} \tag{12}$$

The characteristic polynomial $P(z^{-1})$ is

$$\begin{aligned} P(z^{-1}) &= A(z^{-1})S(z^{-1}) + B(z^{-1})R(z^{-1}) \\ &= p_0 + p_1 z^{-1} + \cdots + p_n z^{-n}. \end{aligned} \tag{13}$$

A model matching method, DCRA, requires a reference model that satisfies the desired time responses. Let such a reference model be $H^*(z^{-1}) = N^*(z^{-1}) / P^*(z^{-1})$. Then the controller {*R, S, T*} is determined such that $H(z^{-1}) \equiv H^*(z^{-1})$. The first step is to solve the following algebraic equation to find the feedback term {R, S} of the controller:

$$A(z^{-1})S(z^{-1}) + B(z^{-1})R(z^{-1}) = P^*(z^{-1}). \tag{14}$$

This identity equation has a unique solution if the following conditions hold:

$$n_{p^*} = n_A + n_S, \quad n_R \geq n_A - 1, \quad \text{and} \quad n_s \geq n_R. \tag{15}$$

To achieve the zero steady state error to a step reference input, the overall system must be of *Type I*. Therefore, the feedforward term $T(z^{-1})$ can be obtained by

$$H(z^{-1})|_{z=1} = \frac{T(1)B(1)}{P(1)} = 1 \quad \Rightarrow \quad T(1) = \frac{P(1)}{B(1)}. \tag{16}$$

Now, the remaining problem is to find a reference model $H^*(z^{-1})$ that meets a prescribed transient response: the maximum overshoot and settling time. Note that the problem of finding $H^*(z^{-1})$ is basically the problem of finding $P^*(z^{-1})$ with a fixed numerator polynomial $N^*(z^{-1})$ if the order of $T(z^{-1})$ is selected to be zero. The DCRA is a very simple method to synthesize such a transfer function model. A practical example applying the DCRA will be presented in section IV.

### *B. A Simple MMAC for $C_q$*

An MMAC structure for the *q-axis* current controller $C_q$ is shown in Fig. 7, where $M_1$, $M_2$, $\cdots$, and $M_N$ denote an individual model of the model bank. There are several ways to construct a model bank. One of the most typical methods is to partition the parameters of the model. Another method is to construct a model bank with models corresponding to several operating points, as used in this approach. Each candidate controller $C_k$ of the controller bank is designed for plant model $M_k$ using DCRA. The design procedure is the same as that described in the previous section. We can see that if the variables, $u$ and $y$, are replaced by $v_q$ and $i_q$, Fig. 7 is equivalent to the feedback system in Fig. 2.

When the PMSM system is changed, the MMAC adapts by determining which model the plant is approaching. The conventional adaptation is based on the residuals between the

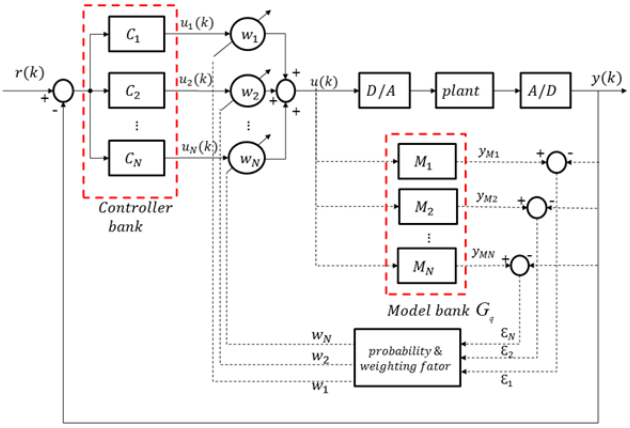


Fig. 7. MMAC structure for the *q-axis* current controller $C_q$

outputs of the models and the plant response.

According to the Bayesian approach [7], the probability of the *jth* model in the model bank being a true model is calculated as

$$p_j(k) = \frac{\exp(-\frac{1}{2}\varepsilon_j^2(k)C_F)p_j(k-1)}{\sum_{i=1}^{N}\exp(-\frac{1}{2}\varepsilon_i^2(k)C_F)p_i(k-1)},\quad (j=1,2,\cdots,N) \tag{17}$$

where $\varepsilon_j(k) = y(k) - y_{Mj}(k)$ is a residual at the $k$th step. Here, $C_F$ is a parameter controlling the convergence rate of $p_j(k)$.

The MMAC is based on the assumption that the plant can be represented by one model of the model bank. However, it is unusual that a single model in the model bank would be exactly equal to the actual system. Hence, suitable weights are assigned to individual control inputs from the controller bank so that models with higher probability are assigned larger weights and vice versa. Such a control input is computed as

$$u(k) = \sum_{j=1}^{N} w_j(k)\cdot u_j(k), \tag{18}$$

where the weighting factor $w_k$ is defined by

$$w_j(k) := \begin{cases} \dfrac{p_j(k)}{\sum_{j=1}^{N} p_j(k)} & for\ \ p_j(k) > \delta_{\min} \\ 0 & for\ \ p_j(k) < \delta_{\min}. \end{cases} \tag{19}$$

In (19), $\delta_{\min}$ is a threshold to limit the importance of past information.

As an alternative method to (18) and (19), we suggest a simple algorithm for weighted control. It was represented in Section II.B that the operating point for the PMSM system can be defined by dividing the *q*-axis current into *N-1* pieces. Since the *q*-axis current can be measured in real time, it is always possible to know both ends of the section to which the current belongs.

Let the *j*th operating point and the *j*th model be $i_{q,j}$ and $M_j$, respectively. It is assumed that when the *q*-axis current goes from $i_{q,j}$ to $i_{q,j+1}$, the dynamic model of the actual system changes linearly from $M_j$ to $M_{j+1}$. Then, the control input is computed as a linear combination of two control inputs, $u_j$ and $u_{j+1}$ if the current value of the *q*-axis current is between the two adjacent operating points, $i_{q,j}$ an $i_{q,j+1}$. That is, at iteration *k*,

$$u(k) = \lambda_j u_j(k) + (1-\lambda_j)u_{j+1}(k),\ \ if\ \ i_{q,j} \le i_q(k) \le i_{q,j+1}, \tag{20}$$
$$(0 \le \lambda_j \le 1,\quad j=1,2,\cdots,N)$$

where a weighting factor $\lambda$ is determined by

$$\lambda_j = \frac{i_q(k) - i_{q,j+1}}{i_{q,j} - i_{q,j+1}},\quad if\ \ i_{q,j} \le i_q(k) \le i_{q,j+1}. \tag{21}$$

Unlike the conventional algorithm in (18), (19), the above algorithm does not require the operation of the probability, and a weighting factor is also computed deterministically. Therefore, this method is referred to as a simple MMAC here.

TABLE I
PARAMETERS OF THE PMSM

| | | |
|---|---|---|
| Rated power | W | 5000 |
| Rated voltage | V | 220 |
| Rated speed | rpm | 3000 |
| Rated torque | N·m | 15.9 |
| Motor inertia | kg·$m^2$ | 42.9x$10^{-4}$ |
| Rated current | A | 23.3 |
| Encoder | point/r | 2000 |

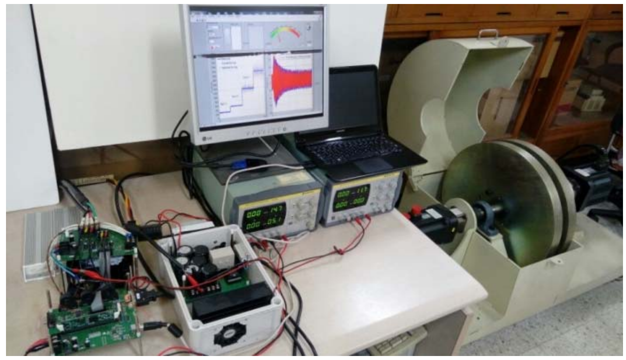

Fig. 8. Experimental setup.

## IV. EXPERIMENTAL RESULTS

The proposed approach was demonstrated by experiments. We used a surface mounted 5 KW PMSM; its parameters are listed in Table I. A flywheel load of 220 kg was mounted on the PMSM with a gear ratio of 5:1, as shown in Fig. 8. A digital controller including SVPWM, Clarke's and Park's transformations were implemented by a DSP (TMS320 F28335, TI) with a clock frequency of 150 MHz. The PMSM was driven by a three phase PWM inverter with an intelligent power module (PS21A7A, 600V, 75A, Mitsubishi). Fig. 9 shows the configuration of the experimental setup.

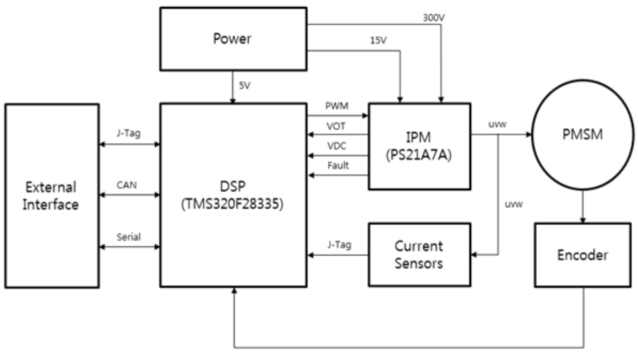


Fig. 9. Configuration of the experimental setup.

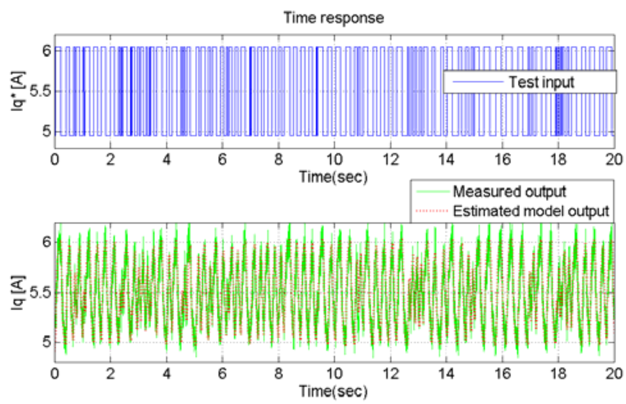


Fig. 10. PRBS test input (upper) applied to the q-axis reference current and its responses (lower): measured output (green) and output of the estimated model (red).

The modeling and design procedures applying the proposed method to this PMSM drive system are given step by step, as follows:

1) First, four operating points of the *q-axis* current were selected and initial controllers were chosen for $C_q$ and $C_d$.
2) Four discrete-time linearized models for $G_q$ and a linearized model for $G_d$ at an operating point were identified using experimental data.
3) Based on these models, an MMAC for $C_q$ and an RST-type digital controller for $C_d$ were designed.
4) A discrete-time linearized model $G_s$ for the speed-control loop including the current controller was obtained using experimental data.
5) Based on this model $G_s$, a digital speed controller $C_s$ was designed using the DCRA.
6) The performance of the overall PMSM drive system was evaluated through various experiments.

### A. Modeling of $G_q$ and $G_d$ in the Current Loop

To build a model bank, we considered four operating points of the *q*-axis currents: 3.5, 4, 5.5, and 7 A, respectively. The corresponding steady state speeds of the motor were about 500, 1000, 2000, and 3000 rpms. Among them, the modelling results of the 5.5 A (about 2000 rpm) case are shown as a sample. The sampling time of the current loop was chosen to be 200 $\mu s$. To identify $G_q$ using a CLID method (CLOE), we selected initial controllers $C_q^o$ and $C_d^o$, as

$S_C^o = 1 - z^{-1}$, $R_C^o = 0.502 - 0.5z^{-1}$, and $T_C^o = 0.002$.

A test input $r = i_q^*$ was generated by adding a PRBS with the amplitude of $\pm 0.55$ to the $r_o = 5.5$ A. The test input and its time response $i_q$ are shown in Fig. 10.

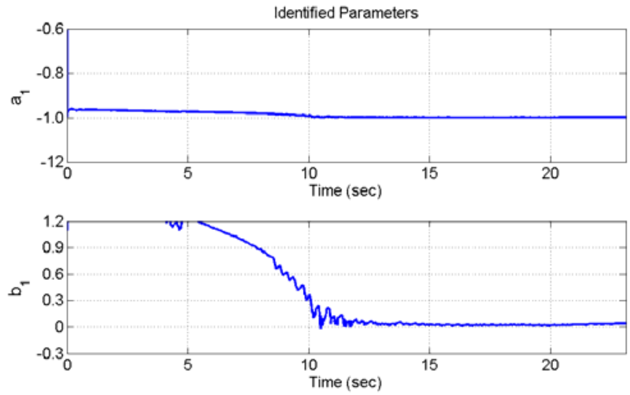


Fig. 11. Estimated parameters of the model (22) at $r_o = 5.5$ A (about 2000 rpm) using the CLOE algorithm.

TABLE II
PARAMETERS OF *Q*-AXIS MODELS $G_q$ IN THE FORM OF (22) ESTIMATED AT FOUR OPERATING POINTS

| *q*-axis models | $M_1$ | $M_2$ | $M_3$ | $M_4$ |
|---|---|---|---|---|
| $r_o = i_{qo}^*$ (A) | 3.5 | 4 | 5.5 | 7 |
| Speed (rpm) | 500 | 1000 | 2000 | 3000 |
| $\hat{a}_{q1}$ | 0.9963 | 0.9974 | 0.998 | 0.996 |
| $\hat{b}_{q1}$ | 0.04726 | 0.05088 | 0.05858 | 0.09786 |

Through the identification process for various order models, we have found that the following first-order model is consistent with the experimental data:

$$\frac{\hat{B}_q(z^{-1})}{\hat{A}_q(z^{-1})} = \frac{\hat{b}_{q1} z^{-1}}{1 + \hat{a}_{q1} z^{-1}} = \frac{0.05858 z^{-1}}{1 - 0.998 z^{-1}}. \tag{22}$$

Fig. 11 shows the convergence of the parameter estimation of model (22), which is obtained by the recursive CLOE algorithm (7). The response (red curve) of the estimated model to the same input is compared with the actual data (green curve) in Fig. 10.

This process was repeated at several operating points to obtain four *q*-axis models in the form of (22), as listed in Table II. The model bank of MMAC consisted of these models.

Similarly, an estimated model for the *d*-axis plant was

TABLE III
PARAMETERS OF FOUR $Q$-AXIS CONTROLLERS IN THE FORM OF (25) DESIGNED FOR THE INDIVIDUAL $Q$-AXIS MODEL $M_k$

| $q$-axis controllers | $C_1$ | $C_2$ | $C_3$ | $C_4$ |
|---|---|---|---|---|
| $r_{ko}$ | 0.6207 | 0.5976 | 0.5289 | 0.2964 |
| $r_{k1}$ | -0.6136 | -0.5910 | -0.5231 | -0.2929 |
| $t_{ko}$ | 0.0071 | 0.0066 | 0.0057 | 0.0034 |

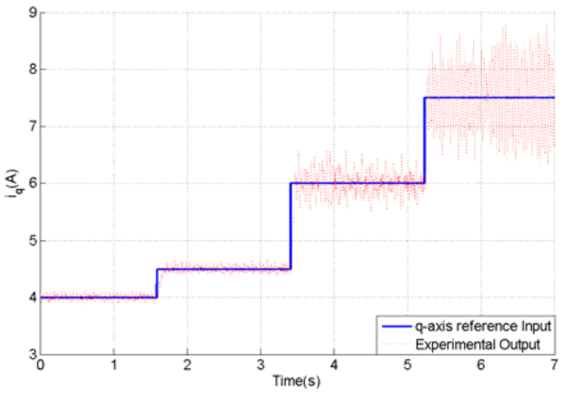


Fig. 12. Tracking performance of the current controller composed of a fixed $C_1$ and a $C_d$ .

obtained at 2000 rpm as follows:

$$\frac{\hat{B}_d(z^{-1})}{\hat{A}_d(z^{-1})}=\frac{\hat{b}_{d1}z^{-1}}{1+\hat{a}_{d1}z^{-1}}=\frac{0.04525z^{-1}}{1-0.984z^{-1}}. \tag{23}$$

*B. Design of Controllers $C_q$ and $C_d$ in the Current Loop*

The design procedure of an MMAC for $C_q$ and an RST-type digital controller $C_d$ will now be described. It is assumed that the current-control system is designed to meet no-overshoot and a settling time of 50 *ms*. Since the current models (22) and (23) are of first-order, the choice of the PI type controllers is sufficient for both current controllers, $C_q$ and $C_d$ . In DCRA, a reference model with the desired transient response can be synthesized by selecting two design parameters: a characteristic ratio ( $\alpha_1$ ), and a generalized time constant ( $\tau$ ). According to the rule [13], a reference characteristic polynomial $P_q^*(z^{-1})$ was selected by

$$P_q^*(z^{-1})=1-1.967z^{-1}+0.9673z^{-2}. \tag{24}$$

We confirmed through simulation that the step response of the reference model $H_q^*(z^{-1})=t_0\hat{B}_q(z^{-1})\big/P_q^*(z^{-1})$ using (24) had no overshoot and the exact settling time of 50 *ms*. If the $q$-axis model is $M_3$ , replacing $P^*(z^{-1})$ of (14) by (24) and solving the algebraic equation (14), we have the following discrete-time PI controller $C_3$ :

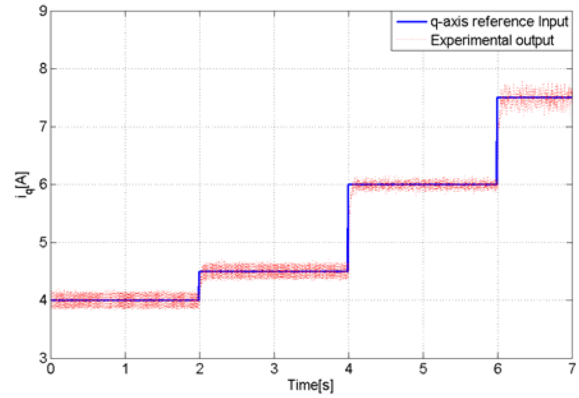


Fig. 13. Tracking performance of the current controller composed of a *q-axis* MMAC and a $C_d$ .

$$\begin{aligned} &S_3(z^{-1})=1-z^{-1},\\ &R_3(z^{-1})=r_{30}+r_{31}z^{-1}=0.5289-0.5231z^{-1},\\ &T_3(z^{-1}):=t_{30}=0.0057. \end{aligned} \tag{25}$$

Repeating this process for other $q$-axis models with the same characteristic polynomial (24) yielded four controllers of the controller bank given in Table III.

The simple adaptation law of (20) and (21) was employed for the $q$-axis MMAC here. The $d$-axis PI controller $C_d$ was designed for the model (23) using the same characteristic polynomial of (24) as for the $q$-axis:

$$\begin{aligned} &S_d(z^{-1})=1-z^{-1},\\ &R_d(z^{-1})=0.3765-0.369z^{-1},\\ &T_d(z^{-1})=0.00749. \end{aligned} \tag{26}$$

We now examine how much the $q$-axis MMAC improves performance compared with using a fixed $q$-axis controller. To do this, we consider a case in which the $q$-axis reference current changes stepwise from 4 A to 4.5, 6, 7.5 A at intervals of about two seconds.

Fig. 12 shows the tracking performance obtained when the current controller was composed of a fixed $q$-axis controller $C_1$ in Table III and a $d$-axis controller $C_d$ in (26). Note that the $q$-axis controller $C_1$ was designed for the model $M_1$ , which is a 3.5A model. Hence, we see that the performance became worse due to nonlinearity as the $q$-axis reference current increased above 6 A.

On the other hand, the current controller composed of a $q$-axis MMAC and a $d$-axis controller $C_d$ in (26) achieved much better performance as shown in Fig. 13. Although the $q$-axis reference current was given as a different value from the predefined operating points (3.5, 4, 5.5, and 7 A), the results showed that the MMAC with (20) and (21) was well adapted.

*C. Modeling of $G_s$ and Design of Controllers $C_s$ in the Speed Feedback Loop*

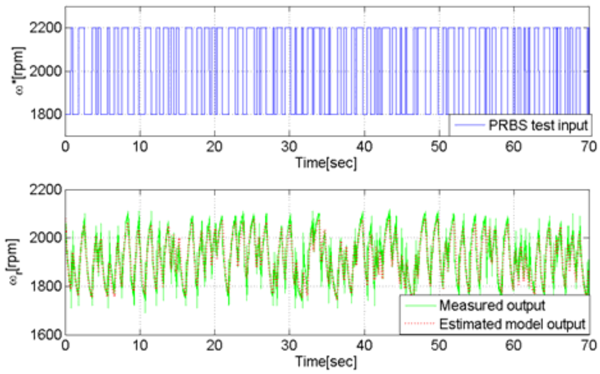

Fig. 14. PRBS test input (upper) and its measured response to speed loop (lower). Estimated model response (red) and experimental output (green).

The current controller described above was implemented by a DSP. As explained in section II.C, the speed-control loop is equivalent to the feedback system shown in Fig. 4. The sampling time for the speed loop was chosen to be 3 *ms* . To make a CLID applicable, a temporary speed controller $C_s^o$ was selected as follows:

$$S_s^o = 1 - 0.5z^{-1},\ R_s^o = 0.1,\ \text{ and } T_s^o = 0.1 .$$

A test input $\omega^*$ was generated by adding 10% PRBS signal to the operating speed of 2000 rpm. This input and its measured response $\omega_r$ are shown in Fig. 14.

Applying the recursive CLOE algorithm to these data, we obtained the following second-order model for $G_s$ :

$$\hat{G}_S = \frac{\hat{B}_S(z^{-1})}{\hat{A}_S(z^{-1})} = \frac{0.1018z^{-1}}{1 - 0.4478z^{-1} - 0.552z^{-2}} . \tag{27}$$

The time response of this estimated model is compared with the actual output in Fig. 14. Parameter estimates using the recursive CLOE method are shown in Fig. 15.

In this example, it was assumed that the speed-control system was designed to satisfy no-overshoot and a settling time of 3 sec. Such time response specifications may be limited by the maximum value of the permissible currents of both Hall sensors and the IPM module. We observed through simulations that it is difficult for this experimental setup to achieve good performance over the full operating speed range if a PID type controller is used. Therefore, a second-order RST controller including an integrator was selected.

According to the method in [13], the reference characteristic polynomial $P_S^*(z^{-1})$ satisfying the above transient response specifications was obtained by

$$\begin{aligned} P_s^*(z^{-1}) = 1 - 1.98585z^{-1} + 0.68155z^{-2} \\ + 0.62267z^{-3} - 0.31829z^{-4}. \end{aligned} \tag{28}$$

We confirmed through simulation that the step response of the reference model $H_s^*(z^{-1}) = {t_0 \hat{B}_s(z^{-1})}/{P_s^*(z^{-1})}$ using (28) had no overshoot and the exact settling time of 3 *sec*. Replacing $P^*(z^{-1})$ of (14) by (28) and solving the algebraic equation (14), we have the following speed controller $C_S$ :

$$\begin{aligned} S_s(z^{-1}) &= (1 - z^{-1})(1 - 0.5767z^{-1}), \\ R_s(z^{-1}) &= 0.38029 - 0.4851z^{-1} + 0.10564z^{-2}, \\ T_s(z^{-1}) &:= t_0 = 0.00076. \end{aligned} \tag{29}$$

This speed controller was implemented in the DSP. Finally, the dynamic response of the overall PMSM drive system was experimentally demonstrated.

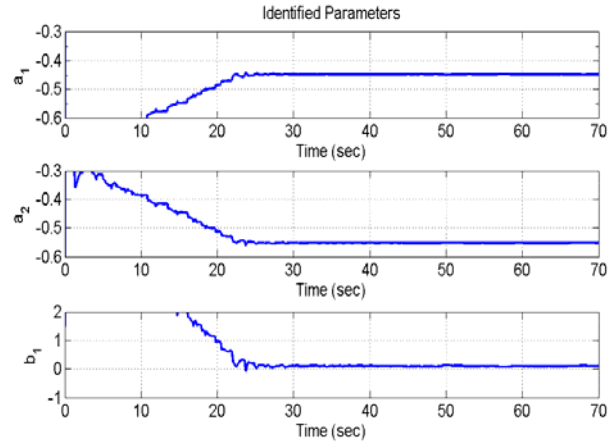

Fig. 15. Parameter estimates of speed model $\hat{G}_s$

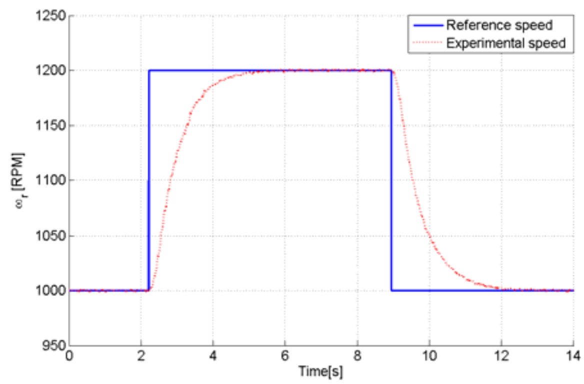

Fig. 16. Experimental result of the overall PMSM control system with a 220kg flywheel load for a variable reference speed.

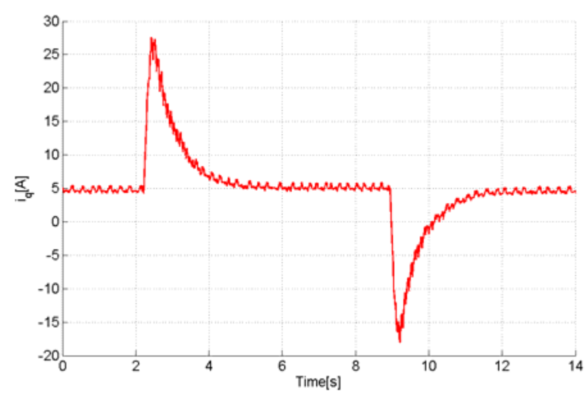

Fig. 17. The *q-axis* current response while the speed control in Fig. 16 is operating.

When the reference speed was changed stepwise from 1000 rpm to 1200 rpm and again to 1000 rpm, the results demonstrated that the proposed controller satisfied the prescribed requirements (i.e., non-overshoot and settling time of 3 sec) exactly, as shown in Fig. 16. Fig. 17 shows the profile of the $q$-axis current during this speed control.

In conclusion, accurate modeling of the vector-controlled PMSM drive system allows the current and the speed controllers to be designed to precisely meet the desired time responses.

## V. CONCLUSIONS

In this paper, we presented an experimental modeling method and a simple MMAC design that satisfies the desired time response specifications for a vector-controlled PMSM drive system. Modeling and design of the controllers are carried out for the following three control loops separately: i) $q$-axis current-control loop, ii) $d$-axis current-control loop, and iii) a speed-control loop. The input-output modeling of the equivalent plant for each control loop is to identify a discrete-time linear model by the CLID method, where experimental data are measured while the subsystem with a temporary controller is being operated.

The rotor speed and electromagnetic torque are dominantly dependent on the $q$-axis current rather than the $d$-axis current. Moreover, the dynamics of the current-control loop has a much faster mode than the speed-control loop due to the large moment of inertia. For these reasons, we have proposed a new controller configuration in which an MMAC is applied to the $q$-axis current control, while a fixed digital controller is applied to the $d$-axis and the speed controls. Apart from the Bayesian approach used in conventional MMAC, a simple algorithm for computing both the weighting factor and the weighted control has been proposed. It is remarkable that the proposed MMAC guarantees robustness from the viewpoint that its performance cannot be worse than the minimal performance of any fixed $q$-axis current controllers.

Once the models are obtained for each loop, the controllers should be designed so that they satisfy the given transient response requirements such as the maximum overshoot and the settling time. We have shown that the DCRA in [10-12] can be applied effectively for this purpose.

Finally, the proposed approach has been demonstrated by experiments. The experimental setup consisted of a surface-mounted PMSM (5 KW, 3 $\phi$ 220V, 8 poles, Higen) equipped with a flywheel load of 220kg, a three phase PWM inverter with an IPM (PS21A7A, 600V, 75A, Mitsubishi), and a digital controller using DSP (TMS320F28335). Modeling for the *q-axis* current loop was performed at four operating points, and it resulted in good outcomes. It was shown that all the experimental responses coincided closely with the design objectives. The accurate modeling of the vector controlled PMSM drive system is remarkable, in that it allows the current and the speed controllers to be designed to satisfy the desired time response requirements precisely. As a result, we expect that the proposed approach can be applied to many actual applications of PMSM.

## ACKNOWLEDGMENT

This work was supported in part by Basic Science Research Program through the National Research Foundation of Korea (NRF) funded by the Ministry of Education [Grant No. NRF-2015R1D1A01060997].

## REFERENCES

[1] H. H. Choi, J. W. Jung, and T. H. Kim, "Digital speed regulator system design for a permanent synchronous motor," *J. Electr. Eng. Tech.*, Vol. 7, No. 6, pp. 911-917, Jun. 2012.

[2] X. Li and S. Li, "Speed control of a PMSM servo system using model reference adaptive control and extended state observer," *Jourla of Power Electronics*, Vol. 14, No. 3, pp.549-563, May 2014.

[3] H. H. Choi, N. T. Vu, and J. W. Jung, "Digital Implementation of an Adaptive Speed Regulator for a PMSM," *IEEE Trans. Power Electron.*, Vol. 26, No.1, pp.911-917, Jan. 2012.

[4] D. Lainiotis, "Patitioning: A unifying framework for adaptive systems, II: Control," *Proc. IEEE*, Vol. 64, No. 8, pp. 1182-1198, Aug. 1976.

[5] K. S. Narendra and J. Balakrishnan, "Adaptive control using multiple models," *IEEE Trans. Autom. Contr.*, Vol. 42, No. 2, pp. 171-187, Feb. 1997.

[6] M. Athans, Y. Baram, D. Castanon, K. P. Dunn, C. S. Green, W. H. Lee, N. R. Sandell Jr., and A. S. Willsky, "Investigation of the multiple model adaptive control (MMAC) method for flight control systems," *NASA Contractor Report 3089*, May 1979.

[7] B. Chaudhuri, R. Majumder, and B. C. Pal, "Application of multiple-model adaptive control strategy for robust damping of interarea oscillations in power systems," *IEEE Trans. Contr. Syst. Tech.*, Vol. 12, No. 5, pp. 727-736, Feb. 2004.

[8] I. D. Landau and A. Karimi, "An output error recursive algorithm for unbiased identification in closed loop," *Automatica*, Vol. 33, No. 8, pp. 933-938, May 1997.

[9] I. D. Landau and Z. Gianluca, "*Digital Control System,*" Springer, 2006.

[10] Y. C. Kim, L. H. Keel, and S. P. Bhattachayya, "Transient response control via characteristic ratio assignment," *IEEE Trans. Autom. Contr.,* Vol. 48, No. 12, pp. 2238-2244, Dec. 2003.

[11] Y. C. Kim and Y. S. Lim, "A Parametric design method of direct digital control with transient response requirement," in *Proc. of the ICCAS-SICE2009*, 2009.

[12] Y. C. Kim, L. Jin, J. Lee, and J. Choi, "Direct digital control of single-phase ac/dc pwm converter system," *Journal of Power Electronics*, Vol. 10, No. 5, pp. 518-527, May 2010.

[13] L. Jin, "Discrete-time characteristic ratio assignment for direct digital control design," Ph.D. dissertation, Chungbuk National Univ., Korea, 2012.

[14] T. Kang, M. Kim, K. Lee, S. Y. Lee, and Y. C. Kim, "Experimental modeling and direct digital control of PMSM," in *Proc. of The 28th Int'l Electric Vehicle Symposium and Exhibition*, 2015.

**Taesu Kang** received the B.S. degree in Information and Communication Eng. and M.S. degree in Electronics Eng. from the Chungbuk National University, Cheongju Korea in 2013 and 2015 respectively. He is working at the Modeling & Simulation team, Defense Research & Development Center, Hanwha Corp., Daejeon Korea as a research engineer. His research interests include HILS, digital control system design for motor drive, and modeling of the precision guidance systems.

**Min-Seok Kim** received the B.S. and M.S. degrees in Electronics Engineering from the Chungbuk National University, Cheongju Korea in 2005 and 2014 respectively. He was a senior researcher at the Samsung Electronics Co. Ltd. from 2005 to 2009 and Research Institute Ubiquitous Bio-Information Technology of Chungbuk National Univ., from 2009 to 2012. He works currently at the Central Research Institute, Korea Hydro & Nuclear Power Co. Ltd., as a research engineer.

**Sa Young Lee** received the B.S., M.S., and Ph.D. degrees in Electrical Engineering from the Myongji University, Seoul Korea, in 1980, 1982, and 1992 respectively. He works with Department of Electrical Eng., Myongji College since 1996 as a professor. His research interests are concentrated on theory and applications of power electronics engineering. He has published many research results in this area.

**Young Chol Kim** received the B.S. from the Korea University, Seoul, Korea in 1981, M.S. and Ph.D. degrees in Electrical Eng. from the Seoul National University, Seoul Korea, in 1983 and 1987, respectively. He has been with the Department of Electronics Eng., Chungbuk National University, Korea since 1988 and is currently a Professor. He was a visiting scholar at Texas A & M University in 1991 and Vanderbilt Univ., Tennessee State University in 2001. He served the president of the Information and Control Society of the Korean Institute of Electrical Engineers (KIEE) from 2009 to 2010. Dr. Kim received Myungsam Ko award from ICROS in 2004, Heungseok Yang award from KIEE in 2012, and multiple awards for outstanding papers. His research interests are in the areas of parametric robust control, dynamic system modeling, low-order controller design for practical industry plants, control system designs for autonomous vehicle, EV, and HEV.